Geophysical Research Letters

RESEARCH LETTER
10.1029/2019GL086124

High Production of Soluble Iron Promoted by Aerosol Acidification in Fog

Jinhui Shi[1,2], Yang Guan[1], Akinori Ito[3], Huiwang Gao[1,2], Xiaohong Yao[1,2], Alex R. Baker[4], and Daizhou Zhang[5]

[1]Key Laboratory of Marine Environmental Science and Ecology, Ocean University of China, Ministry of Education of China, Qingdao, China, [2]Laboratory for Marine Ecology and Environmental Science, Qingdao National Laboratory for Marine Science and Technology, Qingdao, China, [3]Yokohama Institute for Earth Sciences, JAMSTEC, Yokohama, Japan, [4]Centre for Ocean and Atmospheric Sciences, School of Environmental Sciences, University of East Anglia, Norwich, UK, [5]Faculty of Environmental and Symbiotic Sciences, Prefectural University of Kumamoto, Kumamoto, Japan

Key Points:
- Conversion of aerosol Fe from insoluble form to soluble form in fog was much more efficient than in haze and dust
- Underestimation of aerosol soluble Fe in latest models was largely caused by inaccurate simulation under fog conditions
- Proper description of processing of aerosol Fe in fog in models is essential to improve simulations

Supporting Information:
- Supporting Information S1

Correspondence to:
J. Shi and D. Zhang,
dzzhang@pu-kumamoto.ac.jp

Citation:
Shi, J., Guan, Y., Ito, A., Gao, H., Yao, X., Baker, A. R., & Zhang, D. (2020). High production of soluble iron promoted by aerosol acidification in fog. *Geophysical Research Letters*, *47*, e2019GL086124. https://doi.org/10.1029/2019GL086124

Received 4 NOV 2019
Accepted 2 JUN 2020
Accepted article online 9 JUN 2020

Abstract The current poor understanding of soluble iron (Fe) yield in atmospheric aerosols leaves two observational facts having not yet been correctly simulated in numerical models: the high Fe solubility in aerosols with low Fe content and, hence, the wide range of observed Fe solubility. Our observation at Qingdao, a coastal city of China, revealed that soluble Fe was produced along with aerosol acidification much more efficiently in fog than under other weather conditions. The median Fe solubility in fog aerosols, 5.81%, was 3.3 times of that in haze aerosols, 5.2 times of that in clear days, and 21.5 times of that in dust aerosols. Involving fog processing in models may reduce the discrepancy in the atmospheric flux of soluble Fe to the ocean between numerical simulations and field observations.

Plain Language Summary Aerosol soluble Fe depositing into seawater promotes marine primary productivity, alters global ocean carbon storage, and ultimately affects global climate. Current models largely underestimate the concentration of soluble Fe in aerosols, but the reason is not clear. Our present results revealed the high efficiency of fog to drive the conversion of Fe from insoluble form to soluble form in the atmosphere, a process that has been overlooked in models. To increase the simulation accuracy, proper inclusion of fog processing in models is necessary.

1. Introduction

The input of soluble iron (Fe) from the atmosphere into surface seawater via aerosol particle deposition is a key process to promote marine primary productivity and the biological fixation of nitrogen in seawater, alters the distribution of carbon dioxide between the ocean and the atmosphere, and is thus ultimately connected to global climate (Jickells et al., 2005). Soluble Fe in aerosols is derived from the primary emissions of natural and anthropogenic sources (Mahowald et al., 2005; Matsui et al., 2018) and chemical conversions from insoluble Fe in the atmosphere (Ito & Shi, 2016; Meskhidze et al., 2003; Scanza et al., 2018).

Field observations have revealed a very wide range of Fe solubility, the ratio of soluble Fe to total Fe in aerosol particles from 0.02% to 98% in both continental and marine environments, with an inverse hyperbolic relationship between Fe solubility and total Fe content in aerosols; that is, the Fe solubility is generally higher in aerosols with lower Fe content (Sholkovitz et al., 2012). Models with deliberate consideration of aerosol sources and atmospheric processing have successfully captured the inverse relationship, but failed to reproduce the higher values of Fe solubility found by observation and hence the full range of observed solubility. Even the latest models are not able to reproduce the high Fe solubility observed over the Southern Ocean, and the available model-simulated soluble Fe concentration was lower than the observed by a factor of 15 on average (Ito et al., 2019).

The discrepancies between the model simulation results and observations indicate missing sources of Fe-containing aerosols or inadequate processes producing soluble Fe in the models (Meskhidze et al., 2019). By introducing pyrogenic Fe-containing aerosols into models, a recent study improved the comparability of simulated Fe solubility to observations, although the soluble Fe concentration was still underestimated (Ito et al., 2019). We analyzed the total and soluble Fe (defined as dissolved Fe by filtration through 0.45 μm pore-size filters after sonication for 1 hr in ultrapure water) in aerosol particles collected at the coastal city

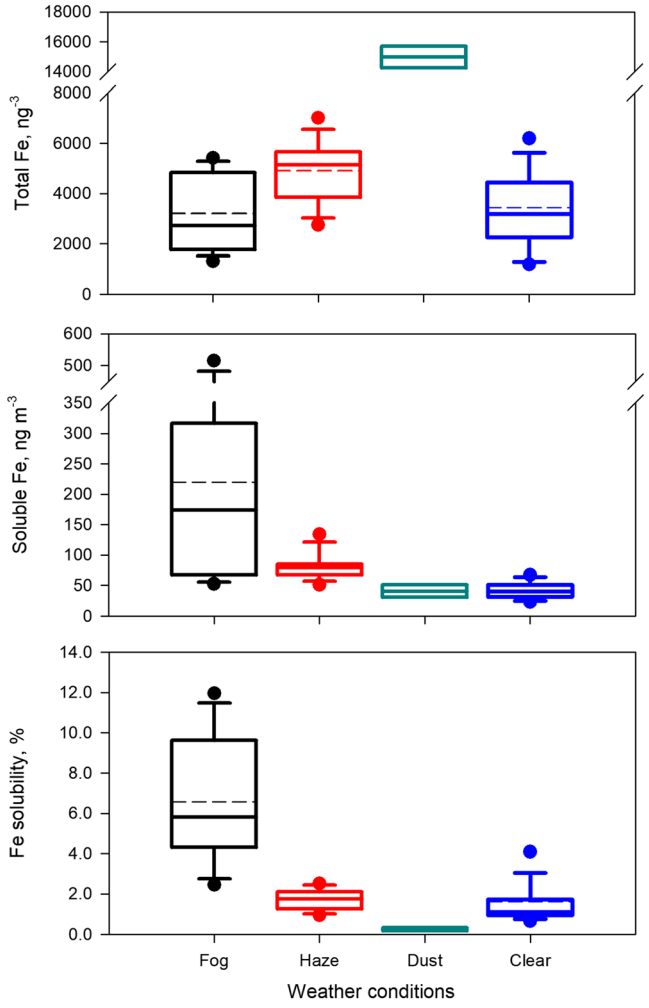

Figure 1. Concentrations of total and soluble Fe and Fe solubility, under fog, haze, dust, and clear-weather conditions. The solid line and the dash line within the box mark the median and the mean, respectively. The boundaries of the box mark the 25th and 75th percentiles. The whiskers above and below the box indicate the 90th and 10th percentiles, and the points indicate the 95th and 5th percentiles.

Qingdao, China, during 4 months when the air was influenced by anthropogenic emissions and episodic desert dust. We found that in fog, Fe was converted from insoluble form to soluble form much more efficiently than under other weather conditions such as haze and dust. Here we report the results and discuss the potential importance of fog processing in the Fe conversion.

2. Methods

Total suspended particle samples were collected between December 2012 and April 2013 on the roof of a building (36°06′N, 120°33′E; 65 m a.s.l.) in the campus of Ocean University of China, about 1 km from the coastline of the Yellow Sea (Figure S1). The collection time for each sample was 24 hr. In total, 112 samples were obtained. In the analysis, each sample filter was divided into 16 equal pieces. For the quantification of total Fe, one piece was digested with 6 ml 15.5 mol L^{-1} HNO_3 + 1.5 ml 22.6 mol L^{-1} HF mixture. The digested solution was evaporated, and then the residue was dissolved in 0.33 mol L^{-1} HNO_3 to 50 ml. For the quantification of soluble Fe, two pieces were subjected to ultrasonic extraction with Milli-Q water. The extract was filtered through a 0.45 μm pore size syringe filter and then digested with 15.5 mol L^{-1} HNO_3. The solution was evaporated, and the residue was dissolved in 0.33 mol L^{-1} HNO_3 to 20 ml. Fe and other metals in the prepared sample solutions were measured using an inductively coupled plasma mass spectrometer (Agilent 7500c ICP-MS). The detection limits of total and soluble Fe were 2 and 0.4 ng m^{-3}, respectively. The relative standard deviations of replicate analysis of the standards were 0.9–4.5%. The digestion recovery of total Fe estimated with a soil sample standard reference material (GSS-8, National Standard Material Centre, China) was 88–105%. Fe content in blank filters was lower than 0.7% of those in the sample filters and was subtracted from the results for each batch. Water soluble ions including SO_4^{2-}, NO_3^-, and oxalate in the aerosol samples were determined using an ion chromatograph. Details of the sample collection, analyses, and quality control are available in Shi et al. (2019) and Text S1.

Weather conditions and the records of fog, haze, and dust during the sample collection were from the China Meteorological Administration. Fog and haze are defined as air turbidity phenomenon with horizontal visibility less than 10 km, in which fog is due to suspended water droplets, and haze is due to suspended mineral, smoke, salt, or their mixing particles. When the duration of fog or haze exceeded 70% of the collection time of a sample, the sample was classified as a fog or haze sample. Air mass backward trajectories calculated from the HYSPLIT model indicate that dust passed on 9 March and 8 April (Figure S2) and the concentration of aluminum as a representative dust element in the samples collected on those days exceeded 10,000 ng m^{-3}, so these samples were classified as dust samples. Samples collected when it was clear and there were no fog, haze, or dust were classified as clear-weather samples. With this classification, there were 19 fog samples, 13 haze samples, 2 dust samples, and 51 clear-weather samples. Here we focus on the results of fog samples in comparison to haze, dust, and clear-weather samples.

3. Results and Discussion

3.1. Fe Content and Solubility

The median concentration of aerosol total Fe was 2,720 ng m^{-3} in fog periods, 5,130 ng m^{-3} in haze episodes, 15,000 ng m^{-3} in dust episodes, and 3,180 ng m^{-3} under clear-weather conditions (Figure 1). The total Fe concentrations differed significantly according to weather conditions, except between fog and clear days ($p < 0.01$, independent sample T test, Table S1). The median concentration of soluble Fe was 174 ng m^{-3}

in fog periods. In contrast, the concentration was 78.8 ng m^{-3} in haze episodes, 40.5 ng m^{-3} in dust episodes, and 40.7 ng m^{-3} under clear-weather conditions. The concentrations of soluble Fe in fog and haze were significantly higher than under dust and clear-weather conditions. However, there was no significant difference in soluble Fe concentration between dust and clear-weather conditions even though the concentration of total Fe in dust episodes was extremely high. Fe in the fog and haze aerosols at Qingdao was mainly from local or regional anthropogenic emissions because of the stable weather conditions (Figure S2). Therefore, the above results indicate high soluble Fe content in anthropogenic particles. This conclusion was supported by the fact that the median concentrations of secondary ions such as SO_4^{2-} and NO_3^- in the fog and haze aerosols were 2.5–3.8 times higher than those under the clear condition. It was also found that the dust did not cause remarkable enhancement of soluble Fe in comparison with the clear condition.

The median Fe solubility in fog aerosols, including droplets and interstitial particles in the fog, was 5.81%, which was 3.3 times higher than in haze aerosols (1.75%), 5.2 times higher than in aerosols in clear days (1.11%), and 21.5 times higher than in dust aerosols (0.27%). Moreover, the Fe solubility had a negative correlation with the visibility ($r = -0.56$, $p < 0.01$, Pearson correlation analysis) and a positive correlation with the relative humidity (RH) ($r = 0.63$, $p < 0.01$) (Figure S3). The low visibility and high RH correspond to foggy weather, while the high visibility and low RH correspond to clear weather.

3.2. Production of Soluble Fe in Fog

There are two processes that can lead to high Fe solubility in aerosol particles: high fraction of soluble Fe in aerosol sources and efficient production of soluble Fe via chemical conversions in the atmosphere (Baker & Croot, 2010; Myriokefalitakis et al., 2015; Zhuang et al., 1992). When fog occurred at Qingdao, the thermodynamic structure of the air was stable, wind was weak, and air movement was stagnant (mean wind speed = 4 m s^{-1}; mean mixing depth = 500 m), which were similar to the situation in haze periods. The chemical composition of aerosol particles in the fog was dominated by particles from local emissions and possibly regional transported ones (Figure S2). If the source of aerosol particles was the reason for the high Fe solubility in fog aerosols, the solubility in the haze aerosols should have been similar to that in the fog aerosols. The much higher solubility in fog suggests that atmospheric processing in fog droplets is the cause of this solubility enhancement.

The major difference between aerosol particles in fog and other weather conditions is the presence of an aqueous layer on particles in the fog, that is, fog droplets. Heterogeneous reactions in aqueous phase media are usually much more efficient than on the surface of dry particles. The aqueous-phase reactions produce acidic species such as sulfate and nitrate (Cartledge et al., 2015) and consequently lead to the acidification of the aerosols and the conversion of Fe from insoluble form to soluble form (Li et al., 2017; Longo et al., 2016; Shi et al., 2015). We simulated the aerosol pH using ISORROPIA-II, a thermodynamic equilibrium model (Text S2), and found that the pH negatively correlated with SO_4^{2-} and NO_3^- and with the molar ratio of the two components to total Fe (Acids/Total-Fe, Acids = $2SO_4^{2-} + NO_3^-$) (Figure S4). The soluble Fe positively correlated with NO_3^- ($r = 0.40$, $p < 0.01$) and SO_4^{2-} ($r = 0.58$, $p < 0.01$), but did not with oxalate. This result suggests that oxalate likely had a limited role in the conversion of aerosol Fe, although oxalate formation enhanced Fe solubility in valley fogwater (Mancinelli et al., 2006; Siefert et al., 1998). One possible reason is that SO_4^{2-} and NO_3^- are the predominant salts produced in the polluted urban air at Qingdao. Another possible reason is that only some Fe-rich particles may contain oxalate (Lin et al., 2019). Because simulated pH was not available for all samples due to the limit of the model (Text S2), we used SO_4^{2-} and NO_3^- to represent the aerosol acidity.

We investigated the correlation of the Fe solubility with Acids/Total-Fe, which was defined as the aerosol relative acidification with respect to Fe (Buck et al., 2006). Results showed that the correlation for fog aerosols largely differed from those for haze and clear-condition aerosols (Figure 2). The slope of the regression line for the fog aerosols was 0.50, while it was about 0.10 for haze, dust, and clear-weather aerosols, indicating a 5 times greater efficiency of Fe conversion in the fog aerosols than in the aerosols under other weather conditions.

The state of aerosol particle surfaces is dependent on the particulate composition and the ambient humidity. Particles containing SO_4^{2-} and NO_3^- usually deliquesce, and the surface changes to wet or liquid state when

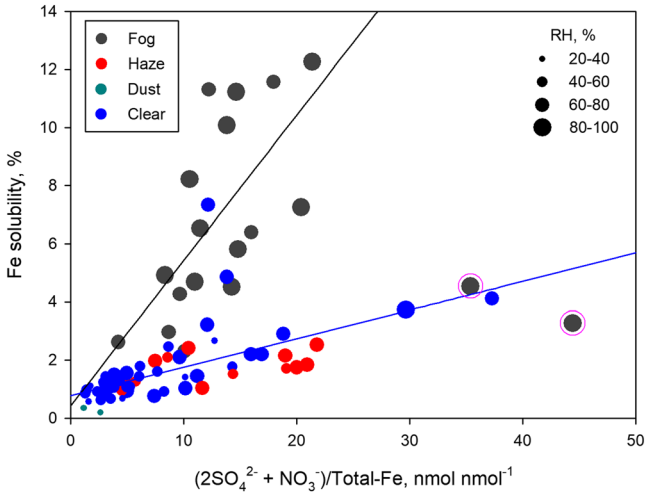

Figure 2. Fe solubility versus ($2SO_4^{2-}$ + NO_3^-)/Total-Fe with respect to relative humidity under fog, haze, dust, and clear-weather conditions. The black line depicts the linear regression for the fog aerosols after excluding the two points outlined with red circles (Y = 0.50X + 0.43, R^2 = 0.44, $p < 0.01$, $n = 17$), and the blue line is the linear regression for the non-fog samples (Y = 0.10X + 0.78, R^2 = 0.39, $p < 0.01$, $n = 66$).

the ambient relative humidity is above 60% (Liu et al., 2017). Particles with wet surfaces readily take up precursor gases that react to produce SO_4^{2-} and NO_3^-, which in turn enable the particles to absorb more water vapor. This positive feedback loop can alter the particles into liquid phase or allow the development of an aqueous layer on the particles with salts, such as SO_4^{2-} and NO_3^-, increasingly produced under humid and polluted conditions. These changes will consequently lead to the increase of soluble Fe in the particles. A laboratory study with simulated cloud-water processes suggested the positive feedback between SO_2 uptake and Fe dissolved on particle surface; that is, SO_2 was oxidized into H_2SO_4 under the catalysis of soluble Fe in mineral aerosols and the H_2SO_4 in return promotes further dissolution of Fe (Wang et al., 2019). In the fog periods of the present study, the RH was about 85% on average and the Acids/Total-Fe was about 15 nmol nmol^{-1} (Figure 2), indicating high aerosol acidification due to the catalysis of soluble Fe and, consequently, substantial production of soluble Fe due to the acidification. Therefore, we suppose that the feedback between the aerosol acidification and Fe catalysis was a major reason for the high Fe solubility in fog aerosols. A recent study showed the formation of soluble Fe catalyzed by some polycyclic aromatic hydrocarbon (PAH) species alone in aerosols (Haynes & Majestic, 2020), but this effect might not be comparable to that of sulfate/nitrate in the present study because PAH contents in Qingdao aerosols was usually at least two orders of magnitude lower than sulfate or nitrate (Guo et al., 2003).

In the cases of haze and clear weather, eight of the 13 haze samples and 19 of the 51 clear-condition samples were collected when the RH > 60%, with the respective average RH of 67% and 68%. The average Acids/Total-Fe was 13 nmol nmol^{-1} in the haze periods and 11 nmol nmol^{-1} under the clear-weather conditions, only slightly lower than that in the fog periods. However, the Fe solubility was about 2%, much lower than that of about 6% in the fog periods. This solubility difference is attributed to the different RH, that is, the greater liquid water content of fog droplets. The RH in the haze and clear days exceeded only a little the point for the particles to deliquesce, reducing the water content in the particles relative to fog droplets. The lower water content in the particles could largely limit the efficiency of the feedback mentioned above. Moreover, the higher dust/liquid ratio due to low water content in particles could lead to lower Fe dissolution rate in acidic solution and consequently suppress the production of soluble Fe (Ito & Shi, 2016).

When the RH was less than 60% ($n = 42$), Fe solubility in the samples was less than 3%, and the solubility of about nine tenths of the samples was even lower than 2% (Figure 2). The particles did not deliquesce, and the dry surface could not promote sulfate and nitrate formation as efficiently as in wet particles. Even in some haze samples that had relatively high ratios of Acids/Total-Fe, the Fe solubility was only about 1.5%, 1.2 times higher than in the clear-weather conditions. These results suggest that the acidification of aerosol particles hardly affected aerosol Fe solubility when RH < 60%, regardless of the large values of Acids/Total-Fe.

3.3. Need for Fog Processes in Models

Numerical models have been developed to simulate the fluxes of total and soluble Fe deposition from the atmosphere to the ocean with various schemes of Fe emission and dissolution. For the dissolution rate in mineral dust, a constant was adopted in early models (Fan et al., 2006). The rate description was updated into the dependence on pH, mineral composition, organic ligands (e.g., oxalate), and solar radiation in later models, and combustion-derived aerosols with enhanced Fe solubility were recently incorporated into models (Ito et al., 2019; Johnson & Meskhidze, 2013; Luo et al., 2008; Myriokefalitakis et al., 2015, 2018; Scanza et al., 2018). These improvements have made the models successful in capturing the major observed trends of soluble Fe at many places. However, even the latest models are not capable of reproducing the high Fe solubility in aerosols with low Fe content and the wide range of the solubility (Ito et al., 2019; Scanza et al., 2018).

Table 1
Comparisons of Total and Soluble Aerosol Fe Concentration (ng m^{-3}) and Fe Solubility (%) Simulated by the IMPACT Model with the Present Observation Data in Fog and Non-Fog Days at Qingdao

	Model			Observation			Model/observation			Soluble
Samples	Total	Soluble	Solubility	Total	Soluble	Solubility	Total	Soluble	Solubility	Fe*
Fog	508 ± 222	9.69 ± 8.78	1.65 ± 1.00	3,210 ± 1,520	220 ± 160	6.57 ± 3.29	0.21 ± 0.21	0.09 ± 0.16	0.28 ± 0.19	49.4 ± 38.4
Non-fog	728 ± 914	16.9 ± 39.2	1.18 ± 1.64	4,080 ± 2,600	50.1 ± 22.5	1.59 ± 1.12	0.20 ± 0.21	0.30 ± 0.56	1.09 ± 1.98	54.4 ± 89.0
All	679 ± 816	15.3 ± 34.8	1.28 ± 1.53	3,880 ± 2,420	88.0 ± 104	2.70 ± 2.77	0.20 ± 0.21	0.26 ± 0.56	0.91 ± 1.98	53.3 ± 80.3

Note. Soluble Fe* (ng m^{-3}) was estimated by multiplying the model estimated Fe solubility with the observed total Fe concentration in the field.

Ito et al. (2019) compared the aerosol Fe solubility simulated by four state-of-the-art models with those observed in multiple field campaigns and reported that the results of the IMPACT model fitted the field data better than the other three models. Here we compare the present data with the 24-hr averaged results simulated with the IMPACT model (2.0° × 2.5°) in the grid cell covering Qingdao. The model-simulated concentrations were lower than our observations on average by 80 ± 21% for total Fe and 74 ± 56% for soluble Fe (Table 1). To identify the possible reason for the discrepancy of the model-simulated soluble Fe from the observed, we tuned the model results of total Fe to fit the observations and investigated how much the corresponding simulated values of soluble Fe could match the observed, which removed the model-observation bias in total Fe concentrations so that differences between simulated and observed soluble Fe concentrations were entirely due to the processes responsible for solubilization of Fe. We multiplied the observed concentration of total Fe by the model simulated Fe solubility and got the corresponding simulated value of soluble Fe, depicted as soluble Fe*. Results showed that the soluble Fe* was 9 ± 198% less than the observed, indicating the model could basically reproduce the soluble Fe concentrations in the aerosols on average. But this apparent agreement was the result of the offset of the largely overestimated soluble Fe* in cases of haze and dust by the largely underestimated soluble Fe* in cases of fog (Figure S5). In fact, the concentration of soluble Fe* in the foggy days (49.4 ng m^{-3} on average) was underestimated by 72 ± 19% compared to the observed.

The model-simulated Fe solubility was further compared with the observed solubility for each sample (Figure 3). All simulated values of Fe solubility in the foggy days were much lower than the observed, with the ratio of the simulated to the observed being far less than 1, indicating a substantial underestimation of Fe solubility by the model under fog conditions. In contrast, 58 of the 66 values for non-fog samples had the ratios close to 1 with the deviations <20%. The simulated values of RH were approximately consistent with the observed RH. However, the simulated values of Acids/Total-Fe differed from and, in particular, were much larger than the observed for the fog and haze periods (Figure 3). With the modeled total Fe tuned to fit the observations, the simulated values of Acids/Total-Fe were consistent with the observed, because

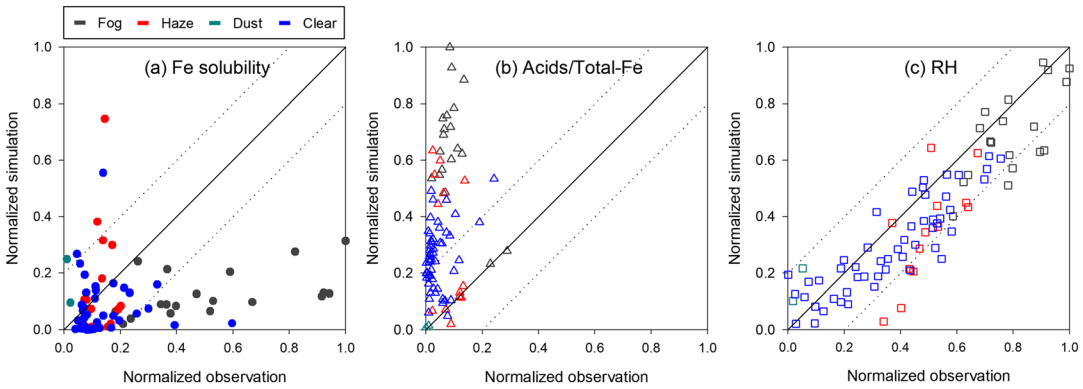

Figure 3. Min-max normalized scatterplots of observations versus simulations for (a) Fe solubility ($r = 0.19$, $p = 0.08$), (b) Acids/Total Fe ($r = 0.66$, $p < 0.01$), and (c) RH ($r = 0.92$, $p < 0.01$). The solid line in each panel shows the 1:1 ratios, and the two dotted lines represent ±20% deviation between the observed and simulated values.

of the low bias between the simulated $2SO_4^{2-} + NO_3^-$ and the observed (Figure S6). These results indicate that the large underestimation of the Fe solubility on average by the model was mainly caused by the inadequate simulation accuracy of the enhancement of Fe solubility under fog conditions, rather than by the lack of enhanced heterogeneous uptake of acidic species and water (Wang et al., 2019). In the present cases, the absence of fog as a special process driving the production of soluble Fe in the model leads to an underestimation of the soluble Fe concentration and the Fe solubility by about 53–91% in the periods of fog (Table 1). Fog is thus a process able to transform Fe from insoluble form into soluble form more efficiently than the current understandings that has so far been overlooked in numerical models.

Fog occurs in various places under certain weather conditions, more frequently over oceans and coastal and mountain areas (Gultepe et al., 2007). We investigated the frequency of fog occurrence in Qingdao from 2010 to 2018 based on the Micaps meteorology data issued by the Chinese Meteorological Administration and found that the annual frequency in days ranged from 17% to 29%. That means the simulated concentration of aerosol soluble Fe at Qingdao in 17–29% days in each year was underestimated, possibly by about 72%. A study on fog occurrence at Chinese Great Wall Station, Antarctica, in the period of 1985–2006 found that the annual frequency at the polar station was about 37% (Yang et al., 2007), showing that fog is also a frequent phenomenon in Antarctica. The Southern Ocean was also affected by mineral dust from southern South America (Patagonia), Australia, and southern Africa, as well as combustion emission from South America and southern Africa (Hara et al., 2019; Ito & Kok, 2017). Regarding the significance of fog in producing soluble Fe indicated by the present results, the inaccurate simulation of soluble Fe production by fog processing is likely the reason for the underestimation of soluble Fe concentrations (and deposition flux) over the Southern Ocean in current model simulations. Therefore, proper incorporation of fog processing for the production of aerosol soluble Fe in models may help to reduce the discrepancy in the atmospheric flux of soluble Fe to the ocean between the results of model simulations and field observations.

4. Summary

We quantified the contents of total and soluble Fe in aerosol samples collected at the coastal city Qingdao, China. Results showed that aerosol soluble Fe in fog aerosols was produced much more efficiently than in haze and dust aerosols, leading to much higher soluble Fe concentration and Fe solubility in fog aerosols than in non-fog aerosols. The comparison with simulated results of the latest improved IMPACT model indicated that the underestimation of aerosol soluble Fe by the model was mainly caused by the inaccurate simulation under fog conditions. The model overestimated the soluble Fe concentration in haze and dust aerosols and compensated somewhat the underestimation due to the absence of the fog enhancement. We propose that fog enhancement is a missing process for the conversion of Fe from insoluble to soluble form in current models, causing a potentially underestimation of aerosol soluble Fe in simulation results. In order to reduce the large discrepancy between model simulation and field observation, proper inclusion of fog enhancement of soluble Fe formation in the models is necessary.

Conflict of Interest

Authors declare no conflict interests.

Data Availability Statement

Data used in the study can be accessed at http://doi.org/10.6084/m9.figshare.10251053.

Acknowledgments

Mr. Xiaoyu Ben assisted sample collection and analyses. This study was funded by the National Key Research and Development Program of China (2016YFC0200504) and the National Nature Science Foundation of China (41876131 and 41430646). D. Z. acknowledges the JSPS Grant No. 16H02942 of Japan. A. I. acknowledges JSPS Grant No. 20H04329 and MEXT Grant No. JPMXD0717935715 of Japan.

References

Baker, A., & Croot, P. (2010). Atmospheric and marine controls on aerosol iron solubility in seawater. *Marine Chemistry*, *120*(1-4), 4–13. https://doi.org/10.1016/j.marchem.2008.09.003

Buck, C. S., Landing, W. M., Resing, J. A., & Lebon, G. T. (2006). Aerosol iron and aluminum solubility in the northwest Pacific Ocean: Results from the 2002 IOC cruise. *Geochemistry, Geophysics, Geosystems*, *7*, Q04M07. https://doi.org/10.1029/2005GC000977

Cartledge, B. T., Marcotte, A. R., Herckes, P., Anbar, A. D., & Majestic, B. J. (2015). The impact of particle size, relative humidity, and sulfur dioxide on iron solubility in simulated atmospheric marine aerosols. *Environmental Science & Technology*, *49*(12), 7179–7187. https://doi.org/10.1021/acs.est.5b02452

Fan, S. M., Moxim, W. J., & Levy, H. II (2006). Aeolian input of bioavailable iron to the ocean. *Geophysical Research Letters*, *33*, L07602. https://doi.org/10.1029/2005GL024852

Gultepe, I., Tardif, R., Michaelides, S. C., Cermak, J., Bott, A., Bendix, J., et al. (2007). Fog research: A review of past achievements and future perspectives. *Pure and Applied Geophysics*, *164*(6-7), 1121–1159. https://doi.org/10.1007/s00024-007-0211-x

Guo, Z. G., Sheng, L. F., Feng, J. L., & Fang, M. (2003). Seasonal variation of solvent extractable organic compounds in the aerosols in Qingdao, China. *Atmospheric Environment*, *37*(13), 1825–1834. https://doi.org/10.1016/S1352-2310(03)00064-5

Hara, K., Sudo, K., Ohnishi, T., Osada, K., Yabuki, M., Shiobara, M., & Yamanouchi, T. (2019). Seasonal features and origins of carbonaceous aerosols at Syowa Station, coastal Antarctica. *Atmospheric Chemistry and Physics*, *19*(11), 7817–7837. https://doi.org/10.5194/acp-19-7817-2019

Haynes, J. P., & Majestic, B. J. (2020). Role of polycyclic aromatic hydrocarbons on the photo-catalyzed solubilization of simulated soil-bound atmospheric iron. *Atmospheric Pollution Research*, *11*(3), 583–589. https://doi.org/10.1016/j.apr.2019.12.007

Ito, A., & Kok, J. F. (2017). Do dust emissions from sparsely vegetated regions dominate atmospheric iron supply to the Southern Ocean? *Journal of Geophysical Research: Atmospheres*, *122*, 3987–4002. https://doi.org/10.1002/2016JD025939

Ito, A., Myriokefalitakis, S., Kanakidou, M., Mahowald, N. M., Scanza, R. A., Hamilton, D. S., et al. (2019). Pyrogenic iron: The missing link to high iron solubility in aerosols. *Science Advances*, *5*(5), eaau7671. https://doi.org/10.1126/sciadv.aau7671

Ito, A., & Shi, Z. (2016). Delivery of anthropogenic bioavailable iron from mineral dust and combustion aerosols to the ocean. *Atmospheric Chemistry and Physics*, *16*(1), 85–99. https://doi.org/10.5194/acp-16-85-2016

Jickells, T. D., An, Z. S., Andersen, K. K., Baker, A. R., Bergametti, G., Brooks, N., et al. (2005). Global iron connections between desert dust, ocean biogeochemistry, and climate. *Science*, *308*(5718), 67–71. https://doi.org/10.1126/science.1105959

Johnson, M. S., & Meskhidze, N. (2013). Atmospheric dissolved iron deposition to the global oceans: Effects of oxalate-promoted Fe dissolution, photochemical redox cycling, and dust mineralogy. *Geoscientific Model Development*, *6*(1), 1901–1947. https://doi.org/10.5194/gmdd-6-1901-2013

Li, W., Xu, L., Liu, X., Zhang, J., Lin, Y., Yao, X., et al. (2017). Air pollution-aerosol interactions produce more bioavailable iron for ocean ecosystems. *Science Advances*, *3*(3), e1601749. https://doi.org/10.1126/sciadv.1601749

Lin, Q., Bi, X., Zhang, G., Yang, Y., Peng, L., Lian, X., et al. (2019). In-cloud formation of secondary species in iron-containing particles. *Atmospheric Chemistry and Physics*, *19*(2), 1195–1206. https://doi.org/10.5194/acp-19-1195-2019

Liu, Y., Wu, Z., Wang, Y., Xiao, Y., Gu, F., Zheng, J., et al. (2017). Submicrometer particles are in the liquid state during heavy haze episodes in the urban atmosphere of Beijing, China. *Environmental Science & Technology Letters*, *4*(10), 427–432. https://doi.org/10.1021/acs.estlett.7b00352

Longo, A. F., Feng, Y., Lai, B., Landing, W. M., Shelley, R. U., Nenes, A., et al. (2016). Influence of atmospheric processes on the solubility and composition of iron in Saharan dust. *Environmental Science & Technology*, *50*(13), 6912–6920. https://doi.org/10.1021/acs.est.6b02605

Luo, C., Mahowald, N., Bond, T., Chuang, P. Y., Artaxo, P., Siefert, R., et al. (2008). Combustion iron distribution and deposition. *Global Biogeochemical Cycles*, *22*, GB1012. https://doi.org/10.1029/2007GB002964

Mahowald, N. M., Baker, A. R., Bergametti, G., Brooks, N., Duce, R. A., Jickells, T. D., et al. (2005). Atmospheric global dust cycle and iron inputs to the ocean. *Global Biogeochemical Cycles*, *19*, GB4025. https://doi.org/10.1029/2004GB002402

Mancinelli, V., Decesari, S., Emblico, L., Tozzi, R., Mangani, F., Fuzzi, S., & Facchini, M. C. (2006). Extractable iron and organic matter in the suspended insoluble material of fog droplets. *Water, Air, and Soil Pollution*, *174*(1-4), 303–320. https://doi.org/10.1007/s11270-006-9118-x

Matsui, H., Mahowald, N. M., Moteki, N., Hamilton, D. S., Ohata, S., Yoshida, A., et al. (2018). Anthropogenic combustion iron as a complex climate forcer. *Nature Communications*, *9*(1), 1593. https://doi.org/10.1038/s41467-018-03997-0

Meskhidze, N., Chameides, W., Nenes, A., & Chen, G. (2003). Iron mobilization in mineral dust: Can anthropogenic SO_2 emissions affect ocean productivity? *Geophysical Research Letters*, *30*(21), 2085. https://doi.org/10.1029/2003GL018035

Meskhidze, N., Völker, C., al-Abadleh, H. A., Barbeau, K., Bressac, M., Buck, C., et al. (2019). Perspective on identifying and characterizing the processes controlling iron speciation and residence time at the atmosphere-ocean interface. *Marine Chemistry*, *217*(20), 103704. https://doi.org/10.1016/j.marchem.2019.103704

Myriokefalitakis, S., Daskalakis, N., Mihalopoulos, N., Baker, A. R., Nenes, A., & Kanakidou, M. (2015). Changes in dissolved iron deposition to the oceans driven by human activity: A 3-D global modelling study. *Biogeosciences*, *12*(13), 3973–3992. https://doi.org/10.5194/bg-12-3973-2015

Myriokefalitakis, S., Ito, A., Kanakidou, M., Nenes, A., Krol, M. C., Mahowald, N. M., et al. (2018). The GESAMP atmospheric iron deposition model intercomparison study. *Biogeosciences*, *15*(21), 6659–6684. https://doi.org/10.5194/bg-2018-285

Scanza, R. A., Mahowald, N. M., Garcia-Pando, C. P., Buck, C., Baker, A., & Hamilton, D. S. (2018). Atmospheric processing of iron in mineral and combustion aerosols: Development of an intermediate-complexity mechanism suitable for Earth System Models. *Atmospheric Chemistry and Physics*, *18*(19), 14,175–14,196. https://doi.org/10.5194/acp-18-14175-2018

Shi, J., Wang, N., Gao, H., Baker, A. R., Yao, X., & Zhang, D. (2019). Phosphorus solubility in aerosol particles related to particle sources and atmospheric acidification in Asian continental outflow. *Atmospheric Chemistry and Physics*, *19*(2), 847–860. https://doi.org/10.5194/acp-2018-892

Shi, Z., Krom, M. D., Bonneville, S., & Benning, L. G. (2015). Atmospheric processing outside clouds increases soluble iron in mineral dust. *Environmental Science & Technology*, *49*(3), 1472–1477. https://doi.org/10.1021/es504623x

Sholkovitz, E. R., Sedwick, P. N., Church, T. M., Baker, A. R., & Powell, C. F. (2012). Fractional solubility of aerosol iron: Synthesis of a global-scale data set. *Geochimica et Cosmochimica Acta*, *89*, 173–189. https://doi.org/10.1016/j.gca.2012.04.022

Siefert, R. L., Johansen, A. M., Hoffmann, M. R., & Pehkonen, S. O. (1998). Measurements of trace metal (Fe, Cu, Mn, Cr) oxidation states in fog and stratus clouds. *Journal of the Air & Waste Management Association*, *48*(2), 128–143. https://doi.org/10.1080/10473289.1998.10463659

Wang, Z., Wang, T., Fu, H., Zhang, L., Tang, M., George, C., et al. (2019). Enhanced heterogeneous uptake of sulfur dioxide on mineral particles through modification of iron speciation during simulated cloud processing. *Atmospheric Chemistry and Physics*, *19*(19), 12,569–12,585. https://doi.org/10.5194/acp-19-12569-2019

Yang, Q., Zhang, L., Xue, Z., & Xu, C. (2007). Analyses of sea fog at Great Wall Station, Antarctica. *Chinese Journal of Polar Research*, *38*(1), 34–38. https://doi.org/10.1002/jrs.1570

Zhuang, G., Yi, Z., Duce, R. A., & Brown, P. R. (1992). Link between iron and sulphur cycles suggested by detection of Fe (II) in remote marine aerosols. *Nature*, *355*(6360), 537–539. https://doi.org/10.1038/355537a0

References From the Supporting Information

Baker, A., Jickells, T., Witt, M., & Linge, K. (2006). Trends in the solubility of iron, aluminium, manganese and phosphorus in aerosol collected over the Atlantic Ocean. *Marine Chemistry*, *98*(1), 43–58. https://doi.org/10.1016/j.marchem.2005.06.004

Chen, Y., Street, J., & Paytan, A. (2006). Comparison between pure-water- and seawater-soluble nutrient concentrations of aerosols from the Gulf of Aqaba. *Marine Chemistry*, *101*(1-2), 141–152. https://doi.org/10.1016/j.marchem.2006.02.002

Fountoukis, C., & Nenes, A. (2007). Isorropia II: A computationally efficient thermodynamic equilibrium model for K^+-Ca^{2+}-Mg^{2+}-NH_4^+-Na^+-SO_4^{2-}-NO_3^--Cl^--H_2O aerosols. *Atmospheric Chemistry and Physics*, *4*(1), 123–152. https://doi.org/10.1023/a:1009604003981

Hsu, S. C., Lin, F. J., & Jeng, W. L. (2005). Seawater solubility of natural and anthropogenic metals within ambient aerosols collected from Taiwan coastal sites. *Atmospheric Environment*, *39*(22), 3989–4001. https://doi.org/10.1016/j.atmosenv.2005.03.033

Hsu, S. C., Wong, G. T. F., Gong, G. C., Shiah, F. K., Huang, Y. T., Kao, S. J., et al. (2010). Sources, solubility, and dry deposition of aerosol trace elements over the East China Sea. *Marine Chemistry*, *120*(1-4), 116–127. https://doi.org/10.1016/j.marchem.2008.10.003

Joos, H., Madonna, E., Witlox, K., Ferrachat, S., Wernli, H., & Lohmann, U. (2017). Effect of anthropogenic aerosol emissions on precipitation in warm conveyor belts in the western North Pacific in winter—A model study with ECHAM6-HAM. *Atmospheric Chemistry and Physics*, *17*(10), 6243–6255. https://doi.org/10.5194/acp-2016-722

Nenes, A., Pandis, S. N., & Pilinis, C. (1998). Isorropia: A new thermodynamic equilibrium model for multiphase multicomponent inorganic aerosols. *Aquatic Geochemistry*, *4*(1), 123–152. https://doi.org/10.1023/a:1009604003981

Shi, J. H., Zhang, J., Gao, H. W., Tan, S. C., Yao, X. H., & Ren, J. L. (2013). Concentration, solubility and deposition flux of atmospheric particulate nutrients over the yellow sea. *Deep Sea Research*, *97*, 43–50. https://doi.org/10.1016/j.dsr2.2013.05.004

Song, S., Gao, M., Xu, W., Shao, J., Shi, G., Wang, S., et al. (2018). Fine-particle pH for Beijing winter haze as inferred from different thermodynamic equilibrium models. *Atmospheric Chemistry and Physics*, *18*(10), 7423–7438. https://doi.org/10.5194/acp-18-7423-2018

Yao, X., Ling, T. Y., Fang, M., & Chan, C. K. (2007). Size dependence of in situ pH in submicron atmospheric particles in Hong Kong. *Atmospheric Environment*, *41*(2), 382–393. https://doi.org/10.1016/j.atmosenv.2006.07.037

Zhang, D., Iwasaka, Y., Shi, G., Zang, J., Hu, M., & Li, C. (2005). Separated status of the natural dust plume and polluted air masses in an Asian dust storm event at coastal areas of China. *Journal of Geophysical Research*, *110*, D06302. https://doi.org/10.1029/2004JD005305

Zhang, X. X., Sharratt, B., Liu, L. Y., Wang, Z. F., Pan, X. L., Lei, J. Q., et al. (2018). East Asian dust storm in May 2017: Observations, modelling and its influence on the Asia-Pacific region. *Atmospheric Chemistry and Physics*, *18*(11), 8353–8371. https://doi.org/10.5194/acp-18-8353-2018